

## Original Article

# Variations of thioredoxin system contributes to increased susceptibility to apoptosis in cardiomyocytes of type 2 diabetic rats

Xiaoqin Zhao<sup>1,2</sup>, Yan Zhang<sup>3</sup>, Xiaoyu Li<sup>4</sup>, Ruiyuan Wang<sup>2</sup>, and Xiangying Jiao<sup>1\*</sup>

<sup>1</sup>Department of Physiology, Key Laboratory of Cellular Physiology, Shanxi Medical University, Taiyuan 030001, China

<sup>2</sup>Graduate School, Beijing Sport University, Beijing 100084, China

<sup>3</sup>Foreign Language Department, Changzhi Medical College, Changzhi 046000, China

<sup>4</sup>Department of Molecular Biology, Shanxi Cancer Hospital, Taiyuan 030013, China

\*Correspondence address. Tel/Fax: +86-351-4135560; E-mail: jiaoxy@gmail.com

**Cardiac complications are the leading cause of death in diabetes. However, the mechanism of diabetes in inducing myocardial injury and apoptosis, and whether the thioredoxin (Trx) system is involved remain unclear. In this study, male Sprague–Dawley rats were randomly divided into two groups: the control and the diabetes groups, and then were randomly divided into five different time-points (the 1st, 2nd, 4th, 12th, and 24th week). The results showed that diabetes-induced cardiac injury was enhanced in the type 2 diabetes rats, as evidenced by aggravated cardiac dysfunction, biochemical indicators, and increased myocardial apoptosis (TUNEL and caspase-3 activity). The activity of myocardial Trx and Trx reductase (TR) in diabetic rats was significantly decreased from the second week and continually aggravated with the disease progression. In diabetic rats, the mRNA expression of *Trx1*, *Trx2*, *TR1*, and *TR2* was decreased first and then increased after the fourth week. Meanwhile, the protein expression of these Trx system members was significantly increased at the 12th week. Trx nitration was cleared, the Trx/ASK1 interaction was significantly decreased, and the activity of p38 was significantly enhanced in cardiac tissues at the 12th week. These results demonstrated that diabetes may cause myocardial injury and apoptosis, and the extent of which was accompanied with the development of the disease. The mechanism is associated with the development of diabetes and the decreased activity of Trx and TR. The reasons for decreased Trx activity may include: decrease of Trx and TR protein expression; nitration modification of Trx; and up-regulation of TXNIP expression.**

**Keywords** diabetes mellitus; cardiomyocyte; apoptosis; thioredoxin

## Introduction

With the improvement of people's living standards, the incidence and mortality of diabetes were significantly increased. Diabetes mellitus (DM) has become a major threat to the health of mankind. Type 2 diabetic (T2DM) is the commonest form of diabetes constituting nearly 90% of the diabetic population in any country. Although people of the middle-aged and the elderly are more likely to develop T2DM, it alarms us that there are an increasing number of young T2DM patients [1]. Among the diabetic complications, cardiac event is the highest risk, and it has become a leading cause of death of diabetes [2]. The resistance of myocardial cells to injury was reduced in diabetes. Human and animal studies have clearly indicated that in the cases of myocardial ischemia and infarction, the heart damage are more severe than non-diabetic patients, as well as with expanded infarct area, increased arrhythmia, and significantly higher mortality rate [3,4]. The mechanisms of diabetic cardiac complications have been studied mainly in the coronary vascular injury, while direct injury to myocardial cells received very little attention.

Thioredoxin (Trx) system is an important protein system in the body, widely expressed in various cells, and plays an important role in the occurrence and development of diseases involving in free radical damage and apoptosis such as inflammation, tumor, and reperfusion injury [5,6]. Diabetes patients show significant glucose and lipid metabolic abnormalities, with generation of a large number of free radicals, including peroxynitrite (ONOO<sup>-</sup>); at the same time, others and our previous researches have shown that there is also apoptosis of myocardial cells [7,8]. Considering that Trx system is an important anti-free radical damage system and can inhibit cell apoptosis *in vivo*, we speculated that Trx might be involved in a variety of damages caused by DM.

Received: October 14, 2013 Accepted: December 17, 2013

Currently, the mechanism of Trx inhibition of cell apoptosis and promoting cell growth is not fully understood, but it is known that Trx may bind with an important intracellular pro-apoptotic protein, apoptosis signal regulating kinase 1 (ASK1) to inhibit and then reduce the occurrence of apoptosis [9,10]. The anti-apoptotic effect of Trx may be due to its chemical modification. Our previous studies have demonstrated that Trx plays a very important role in cell apoptosis induced by myocardial ischemia–reperfusion injury, through generation of a large number of ONOO<sup>-</sup>, which can cause the nitration of the tyrosine<sup>49</sup> of Trx [11,12]. The nitrated Trx loses the ability to bind with ASK1, while free ASK1 could then activate the downstream of c-Jun N-terminal kinase (JNK) and p38 kinase, the two important apoptosis induction kinase systems, to induce apoptosis. Trx interacting protein (TXNIP) is a physiological, internal Trx regulatory protein, which may bind with Trx, and the bound Trx loses the inhibition of cell apoptosis, thereby increasing cell apoptosis.

Therefore, the aims of the present study were as follows: (i) to observe the extent of myocardial injury and apoptosis and to analyze its possible mechanisms in streptozotocin (STZ)-induced T2DM rats at different timepoints; (ii) to determine whether Trx activity is reduced in the T2DM heart; (iii) to identify the mechanism responsible for diabetes-induced Trx alteration; and (iv) to determine the signaling mechanism by which reduced Trx activity leading to apoptotic cardiomyocyte death in the T2DM heart.

## Materials and Methods

### Animals

The investigations conformed to the ‘Guiding Principles in the Use and Care of Animals’ published by the National Institutes of Health (NIH publication no. 8523, revised 1996), and were approved by the Institutional Animal Care and Use Committee of Shanxi Medical University. The 2- to 3-month-old male Sprague–Dawley rats were obtained from Shanxi Medical University.

### Experimental protocol

The T2DM rats were subjected to a high-sugar and a high-fat diet and an STZ injection [40 mg/kg, intraperitoneally (i.p.)] [13]. The control rats (controls) were given only normal diet and equal amount of citric acid buffer injection. One week after injection, fasting blood glucose (FBG) from tail vein blood was measured with FBG  $\geq$  16.7 mM [14], and no significant blood sugar decrease was observed, indicating successful establishment of the T2DM model of rats.

Male Sprague–Dawley rats were randomly divided into two groups: the control group (control), the diabetes group (T2DM). Then the rats in the control group and the T2DM group were randomly divided into five groups of different

time points (the 1st, 2nd, 4th, 12th, and 24th week), with 10 in each group. Four rats died during the experiment, leaving 46 in the T2DM group and 50 in the control group.

### Determination of blood glucose and insulin

At the beginning of feeding, 1 week after STZ treatment, and at different time points after STZ injection (the 1st, 2nd, 4th, 12th, and 24th week), the blood samples were collected, respectively, from the tail vein of the rats that had been fasted overnight, and the blood glucose was measured by the OneTouch blood glucose meters (Johnson & Johnson, New Brunswick, USA). The blood samples were centrifuged at 6750 g for 10 min and the plasma was drawn off. The serum was analyzed spectrophotometrically using insulin ELISA kit (ADL, New York, USA) to determine the level of insulin according to the manufacturer’s instructions.

### Determination of ventricular function *in vivo*

At the different time points, the rats were sacrificed in batches and the indicators of cardiac function *in vivo* were measured. Following anesthesia with intravenous injection of urethane (20%, 1 g/kg), the heart was exposed via a median line left thoracotomy and a catheter was inserted into the left ventricle through the ventricular wall for measurement of the left ventricular pressure [15]. Left ventricular systolic pressure (LVSP), left ventricular diastolic pressure, left ventricular end-diastolic pressure, and maximal rate of rise and decline of ventricular pressure ( $\pm dP/dt_{\max}$ ) were obtained by MS 2000 Bio-Signal analysis system (Chengdu Taimeng Technology Co., Ltd, Chengdu, China). While the chest was open, the pleurae was not destroyed, thus autonomic respiration was maintained.

### Determination of serum creatine kinase-MB and cardiac troponin I activity

Arterial blood samples were collected before the rats were sacrificed in all the groups. Samples were centrifuged at 6750 g for 10 min and the plasma was drawn off. The serum was analyzed spectrophotometrically for creatine kinase-MB (CK-MB) and cardiac troponin I (cTnI) activity according to the manufacturer’s instructions.

### Determination of caspase-3 protease activity and myocardial apoptotic death

The substrates Ac-DEVD-AFC, Ac-IETC-AFC, and Ac-LEHD-AFC were used, respectively, to determine the caspase (-3, -8, and -9) protease activity according to the manufacturer’s instructions (Biomol, Houston, USA) [16]. Myocardial tissue was homogenized in ice-cold lysis buffer and then centrifuged at 27,000 g for 10 min at 4°C. The supernatant (50 ml) was harvested and incubated with a buffer containing 10 mM dithiothreitol (DTT) and 5 ml of the substrate (the final concentration is 200 mM) at 37°C for

1.5 h. The activity of caspase was determined using a spectrophotometer at 405 nm (SpectraMax M2e, Molecular Devices, Sunnyvale, CA, USA) and the AFC content can be calculated with the AFC standard curve. Caspase activity can be calculated as:  $[AFC (90 \text{ min}) - AFC (0 \text{ min})] / \text{protein loaded} / 1.5 \text{ h}$ .

An *in situ* cell death detection kit (Roche, Basel, Switzerland) was used to examine myocardial apoptosis as reported previously [17]. Briefly, the transmural myocardial tissues were fixed with 4% paraformaldehyde in phosphate-buffered saline and embedded in paraffin. The TUNEL staining was then performed on the paraffin slides according to the manufacturer's protocol. Apoptosis index was assessed by measuring the percentage of apoptotic nuclei in each slide.

### Determination of Trx activity

Trx activity was determined by using the insulin disulfide reduction assay [18,19]. Briefly, 160  $\mu\text{g}$  of myocardial tissue extracts were pre-incubated at 37°C for 20 min with 4  $\mu\text{l}$  activation buffer [50 mM 4-(2-Hydroxyethyl) piperazine-1-ethanesulfonic acid (HEPES), 1 mM ethylenediaminetetraacetic acid (EDTA), 1 mg/ml bovine serum albumin (BSA), and 2 mM DTT] to reduce Trx. After the addition of 20  $\mu\text{l}$  reaction buffer (250 mM HEPES, 10 mM EDTA, 2 mg/ml NADPH, and 6 mg/ml insulin), the reaction was started by the addition of mammalian Trx reductase (TR, 4  $\mu\text{l}$ , 3 U/ml; Sigma, St Louis, USA) or water as a control, and the samples were incubated for 1 h at 37°C. The reaction was terminated by adding 125  $\mu\text{l}$  of stopping solution [0.5 M Tris-HCl, 6 M guanidine-HCl and 4 mg/ml 3-carboxy-4-nitrophenyl disulfide, and 0.4 mg/ml 5, 5'-dithiobis(2-nitrobenzoic acid) (DTNB)] and the absorption values were measured at 412 nm.

### Determination of TR activity

TR reduces DTNB using reducing equivalents from NADPH. The product in the reaction, 5'-thionitrobenzoic acid, is yellow and has a maximum absorbance at 412 nm. The reduction of DTNB was used to determine TR activity using Thioredoxin reductase assay kit (Cayman, Ann Arbor, MI, USA) according to the manufacturer's instructions.

### Detection of Trx system mRNAs by real-time quantitative polymerase chain reaction

Analysis of gene expression was carried out by using real-time quantitative polymerase chain reaction (PCR) with SYBR green (Sigma) in the Mx3005 real-time PCR system (Stratagene, Cedar Creek, USA). Total RNA was extracted from cardiac tissue using the Trizol reagent (Invitrogen, Carlsbad, USA). Total RNA (3 mg) was reversely transcribed into cDNA. The thermal profile for real-time quantitative PCR was 95°C for 30 s, followed by 40 cycles of 95°C for 5 s, and 60°C for 20 s. The primer sequences were shown in Table 1.

Samples were normalized to *GAPDH* expression to ensure equal loading. The specificity of the amplified product was monitored by its dissociation curve. The results, expressed as the fold difference in the number of target gene (*Trx1*, *Trx2*, *TR1*, *TR2*, or *TXNIP*) copies relative to the number of *GAPDH* gene copies, were determined by the relative quantitative  $2^{-\Delta\Delta\text{Ct}}$  method [20], using the following equations:  $\Delta\Delta\text{Ct} = \Delta\text{Ct} (\text{target gene}) - \Delta\text{Ct} (\text{GAPDH})$ , where  $\Delta\text{Ct} (\text{target gene}) = \text{Ct} (\text{experimental target gene}) - \text{Ct} (\text{control target gene})$  and  $\Delta\text{Ct} (\text{GAPDH}) = \text{Ct} (\text{experimental GAPDH}) - \text{Ct} (\text{control GAPDH})$ .

### Detection of Trx system proteins by western blot analysis

Myocardial tissue was saved for the analysis of Trx system proteins using western blot analysis. Briefly, cardiac tissue (50 mg) was lysed, and then homogenated to extract the total protein. Protein concentration in the supernatant was determined using BCA kit (Pierce, Rockford, USA). Total protein (50  $\mu\text{g}$ ) was loaded on a 10% sodium dodecyl sulfate–polyacrylamide gel electrophoresis (SDS–PAGE), electrophoresed, and transferred onto nitrocellulose membrane. After being blocked with 5% BSA at room temperature for 2 h, the membrane was incubated with primary antibody overnight at 4°C (Trx1: 1 : 7500, Millipore, Billerica, USA, #AB9328; Trx2: 1 : 1000, Abcam, Cambridge, UK, #ab16838; TR1: 1 : 5000, Millipore, #07-613; TR2: 1 : 2000, Abcam, #ab16841; and TXNIP: 1 : 1250, Invitrogen, #40-3700), and then incubated with the horseradish

**Table 1. The primers used in this study**

Gene	Forward primer	Reverse primer	Gene ID
<i>Trx1</i>	5'-CGTAAATGCATGCCGACCTTC-3'	5'-AGGCAAACCTCCGTAATAGTGGCTTA-3'	116484
<i>Trx2</i>	5'-CGGACATTTACACCACCAGAG-3'	5'-CCGTGCTGTTTGGCTACCATC-3'	79462
<i>TR1</i>	5'-CAAATTTCCGGCAGTGTGTGTC-3'	5'-GAGCCATGCAATGGAGTCTGAGTA-3'	58819
<i>TR2</i>	5'-AGGACGTGGGCACCTTTGAC-3'	5'-GGTTGGTATTAACGCCAGCCTTC-3'	50551
<i>TXNIP</i>	5'-GGCAATCAGTAGGCAAGTCTCCA-3'	5'-TTCCGACATTCACCCAGCAA-3'	117514

peroxidase-conjugated anti-rabbit IgG (Cell Signaling, Beverly, USA). The membrane was developed with a SuperSignal chemiluminescent detection kit (Pierce) and visualized with a Kodak Image Station 400 (Rochester, USA). The blot densities were analyzed with Kodak 1D software (version 3.6) [21].

### Detection of Trx nitration formation

Tissue block was lysed and homogenized. The protein concentration in the supernatant was determined using BCA kit. Briefly, 60  $\mu$ l of protein A agarose beads was mixed with 200  $\mu$ l of binding buffer containing 8  $\mu$ l of a monoclonal antibody against Trx1 (OriGene, Rockville, USA), then incubated with gentle rocking at 4°C for 1 h. The mixture was mixed with 400  $\mu$ g of sample protein and binding buffer to a total volume of 500  $\mu$ l, and was subsequently rocked gently overnight at 4°C. The mixtures were centrifuged at 31,500 g for 2 min and the supernatant was discarded. Then, 500  $\mu$ l of binding buffer was added and the mixture was mixed upside down about 10 times, subsequently being centrifuged at 31,500 g for 2 min. The supernatant was drawn off, and the agarose beads were washed three times with binding buffer. Finally, 20  $\mu$ l of the sample buffer was added to the agarose beads, mixed and heated at 95°C for 5–10 min, and then the extract was subjected to a conventional SDS–PAGE. Trx nitration formation was measured by western blot analysis using a monoclonal antibody against nitrotyrosine followed by enhanced chemiluminescent detection.

### Detection of Trx/ASK1 interaction

Cardiac tissue was homogenized with lysis buffer. Immunoprecipitation and immunoblotting were performed according to the procedure described by Vadseth *et al.* [22]. In brief, endogenous Trx1 was immunoprecipitated with an anti-rat Trx1 monoclonal antibody (OriGene). After sample separation, the Trx1/ASK1 interaction was determined by using a polyclonal antibody against ASK1 (Upstate, Billerica, USA). The blot was developed with SuperSignal-Western reagent (Pierce) and visualized with a Kodak Image Station 400. The blot densities were analyzed with Kodak 1D software (version 3.6).

### Detection of p38 kinase activity

The p38 kinase activity was analyzed by using a p38 assay kit (Cell Signaling) with activating transcription factor-2 (ATF-2) as a substrate according to the manufacturer's instruction [23]. Briefly, heart tissue was homogenized in ice-cold cell lysis buffer. The equivalent lysates were immunoprecipitated with a monoclonal antibody against phospho-p38 kinase (Thr180/Tyr182) in order to separate the activated p38 kinase. The p38 kinase was incubated with ATF-2, then the mixture was separated by SDS–PAGE, and

ATF-2 phosphorylation was measured by western blotting using a monoclonal antibody against phosphorylated ATF-2 followed by enhanced chemiluminescent detection.

### Statistical analysis

All data were presented as the mean  $\pm$  SD and analyzed by using SPSS 15.0 software. To calculate the difference between the two groups, unpaired Student's *t*-test was used. For datasets of more than two groups, one-way analysis of variance was used followed by Bonferroni's test. A value of  $<0.05$  was considered statistically significant.

## Results

### The successful establishment of T2DM rat model

After 1 week STZ treatment, the level of blood glucose in rats of the T2DM group became significantly higher than that of the control group; meanwhile, the serum insulin level of the T2DM group was not significantly different from that of the control group, even higher at the 24th week (Table 2). This suggested that the T2DM rat model was successfully established.

### T2DM enhanced myocardial injury

Using a Millar Mikro-Tip catheter and pressure transducer, direct cardiac function index, LVSP, and  $\pm dP/dt_{max}$  values were obtained. To fully realize the characters of myocardial injury in T2DM, time-dependent alteration of hemodynamics among the experimental groups were detected. As shown in Table 3, the cardiac function in the T2DM group was aggravated at the 12th and 24th weeks, compared with those of the control group; the levels of LVSP and  $\pm dP/dt_{max}$  in the T2DM group were significantly decreased, and became lower as the disease progressed. Biochemical indicators (shown in Table 4) were compared with that of the control

**Table 2. Changes of blood glucose and serum insulin**

Time (week)	Group	<i>n</i>	Blood glucose (M)	Serum insulin (ng/ml)
1	Control	10	5.40 $\pm$ 0.20	0.17 $\pm$ 0.02
	T2DM	10	16.90 $\pm$ 1.80**	0.25 $\pm$ 0.02
2	Control	10	5.30 $\pm$ 0.30	0.24 $\pm$ 0.02
	T2DM	10	17.10 $\pm$ 1.90**	0.28 $\pm$ 0.03
4	Control	10	5.30 $\pm$ 0.40	0.57 $\pm$ 0.03
	T2DM	10	17.20 $\pm$ 1.70**	0.56 $\pm$ 0.04
12	Control	10	5.50 $\pm$ 0.30	0.49 $\pm$ 0.02
	T2DM	10	17.80 $\pm$ 1.90**	0.45 $\pm$ 0.02
24	Control	10	5.30 $\pm$ 0.20	0.45 $\pm$ 0.02
	T2DM	6	22.70 $\pm$ 1.80**	0.68 $\pm$ 0.05**

\*\**P* < 0.01 vs. control.

**Table 3. Changes of indicators for cardiac function**

Time (week)	Group	<i>n</i>	LVSP (kPa)	+dP/dt <sub>max</sub> (kPa/s)	−dP/dt <sub>max</sub> (kPa/s)
1	Control	10	15.41 ± 2.06	615.99 ± 123.51	648.10 ± 134.62
	T2DM	10	16.21 ± 1.14	655.80 ± 144.56	708.66 ± 189.22
2	Control	10	16.56 ± 1.38	602.66 ± 110.26	632.52 ± 146.98
	T2DM	10	15.31 ± 1.85	597.28 ± 128.56	640.02 ± 153.37
4	Control	10	16.81 ± 2.37	593.01 ± 100.26	676.44 ± 174.23
	T2DM	10	16.49 ± 2.78	618.68 ± 147.63	698.56 ± 140.10
12	Control	10	16.10 ± 1.28	596.91 ± 143.68	607.74 ± 165.41
	T2DM	10	13.74 ± 1.69**	456.49 ± 168.95*	475.74 ± 172.54*
24	Control	10	16.79 ± 1.86	607.36 ± 149.52	575.39 ± 176.32
	T2DM	6	12.56 ± 2.12**	432.85 ± 186.43*	453.28 ± 194.58*

LVSP, left ventricular systolic pressure; +dP/dt<sub>max</sub>, maximal rate of rise and decline of ventricular pressure; −dP/dt<sub>max</sub>, maximal rate of rise and decline of ventricular pressure.

\**P* < 0.05.

\*\**P* < 0.01 vs. control.

**Table 4. Changes of biochemical indicators on myocardial injury**

Time (week)	Group	<i>n</i>	CK-MB (ng/ml)	cTnI (ng/ml)
1	Control	10	14.89 ± 2.82	0.24 ± 0.04
	T2DM	10	18.03 ± 2.89	0.30 ± 0.08
2	Control	10	11.62 ± 0.99	0.30 ± 0.07
	T2DM	10	23.67 ± 3.02**	0.57 ± 0.09
4	Control	10	11.78 ± 1.29	0.72 ± 0.19
	T2DM	10	24.53 ± 1.79**	1.70 ± 0.20*
12	Control	10	11.48 ± 1.66	0.77 ± 0.10
	T2DM	10	25.07 ± 4.07**	1.50 ± 0.25*
24	Control	10	12.62 ± 1.19	0.24 ± 0.02
	T2DM	6	20.82 ± 1.36	0.46 ± 0.13*

CK-MB, creatine kinase-MB; cTnI, cardiac troponin I.

\**P* < 0.05.

\*\**P* < 0.01 vs. control.

group. CK-MB content in the T2DM group was significantly increased at the 2nd, 4th, and 12th week, suggesting that it was increased with the disease progression; cTnI content in the T2DM group was also significantly increased at the 4th, 12th, and 24th week, suggesting that it was also increased when the disease was prolonged.

### T2DM enhanced myocardial apoptotic cell formation

To analyze the myocardial apoptosis, both caspase-3 activity assay and TUNEL staining were carried out. The results showed that caspase-3 activity in the T2DM group was significantly increased at the 4th and 12th week when compared with that of the control group (**Fig. 1A**); caspase-8 activity in the T2DM group was significantly increased at

the 4th and 12th week (**Fig. 1B**); while caspase-9 activity in the T2DM group was also significantly increased at the 12th and 24th week (**Fig. 1C**). Myocardial apoptosis became obvious after 12 weeks of STZ injection as shown in the caspase-3 activity assay, so we only used TUNEL staining to detect the heart samples at the 12th week. The results showed that a very low number of TUNEL-positive cells were observed in myocardial tissues from the control rats, while a significantly high number of TUNEL-positive cells were observed in myocardial tissues from the 12th week T2DM rats (**Fig. 1D**).

### The activity of Trx and TR in T2DM rats was decreased

The activity of Trx system might be related to the enhancement of myocardial apoptosis in T2DM rat. Compared with the control group, Trx activities in T2DM rats were decreased at the 2nd, 4th, 12th, and 24th week, and continuously decreasing with the development of the disease (**Fig. 2A**). TR activities of T2DM rats were also significantly decreased at the 2nd, 4th, 12th, and 24th week, and continuously decreasing with the development of the disease (**Fig. 2B**).

### The change of mRNA and protein expression of Trx system in the T2DM heart

In order to find the reasons for the decline of the Trx and TR activities, the mRNA and protein expression levels were detected. The results showed that compared with those of the control group, the mRNA expression levels of *Trx1*, *Trx2*, *TR1*, and *TR2* in the T2DM group were not significantly different at the 1st and 2nd week, while decreased at the 4th week, increased at the 12th week, and decreased at the 24th week. The differences were of statistical significance except

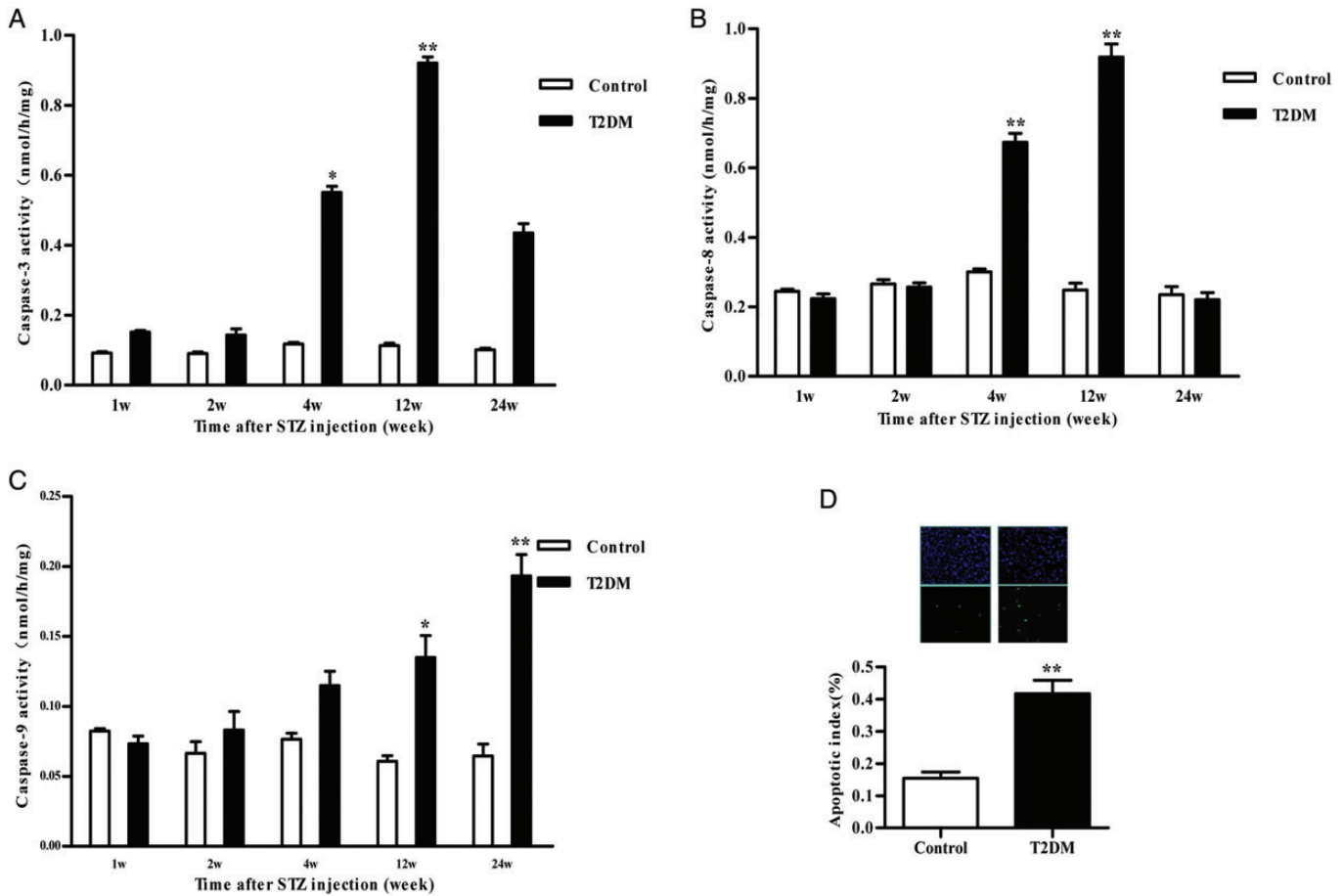


**Figure 1. Cell apoptosis in myocardial tissue in diabetic rats** (A) Caspase-3; (B) caspase-8; (C) caspase-9 activity; and (D) TUNEL labeling in the heart of control and T2DM rats. All values are expressed as the mean  $\pm$  SD. In the T2DM group at week 24,  $n = 6$ ; and in the rest groups,  $n = 10$ . \* $P < 0.05$ , \*\* $P < 0.01$  vs. control group.

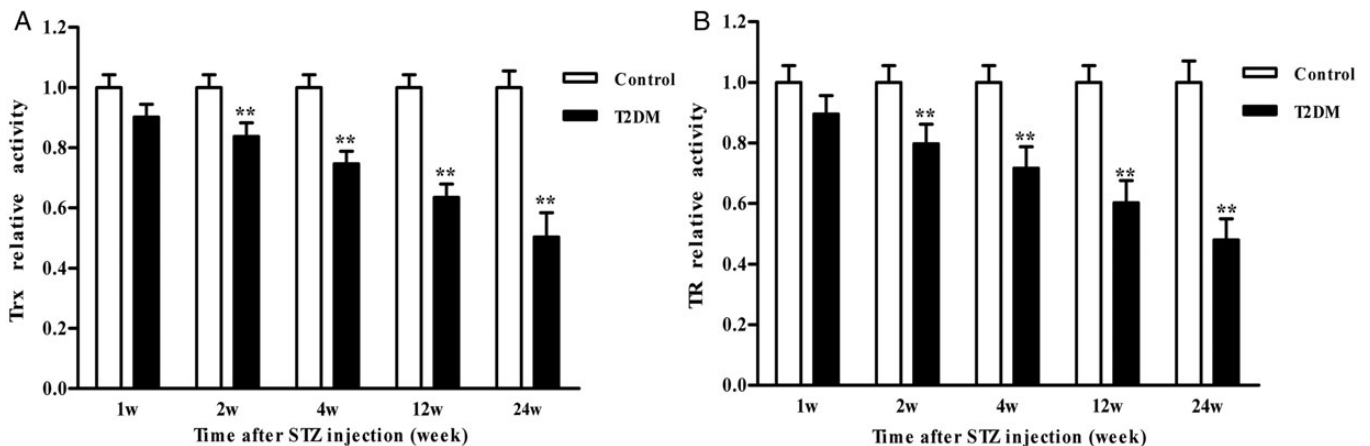


**Figure 2. Trx and TR activity in myocardial tissue in diabetic rats** (A) Trx and (B) TR activity are reduced significantly in the T2DM group compared with the control group. Trx, thioredoxin; TR, Trx reductase. All values are expressed as the mean  $\pm$  SD. In the T2DM group at week 24,  $n = 6$ ; and in the rest groups,  $n = 10$ . \*\* $P < 0.01$  vs. control group.

those of TR1 and TR2 at the 24th week (Fig. 3). Moreover, western blot analysis was used to detect the expression of each protein in the cardiac muscles at the 12th week.

Compared with those of the control group, the protein expression levels of Trx1, Trx2, TR1, and TR2 in the T2DM group were significantly increased (Fig. 4).

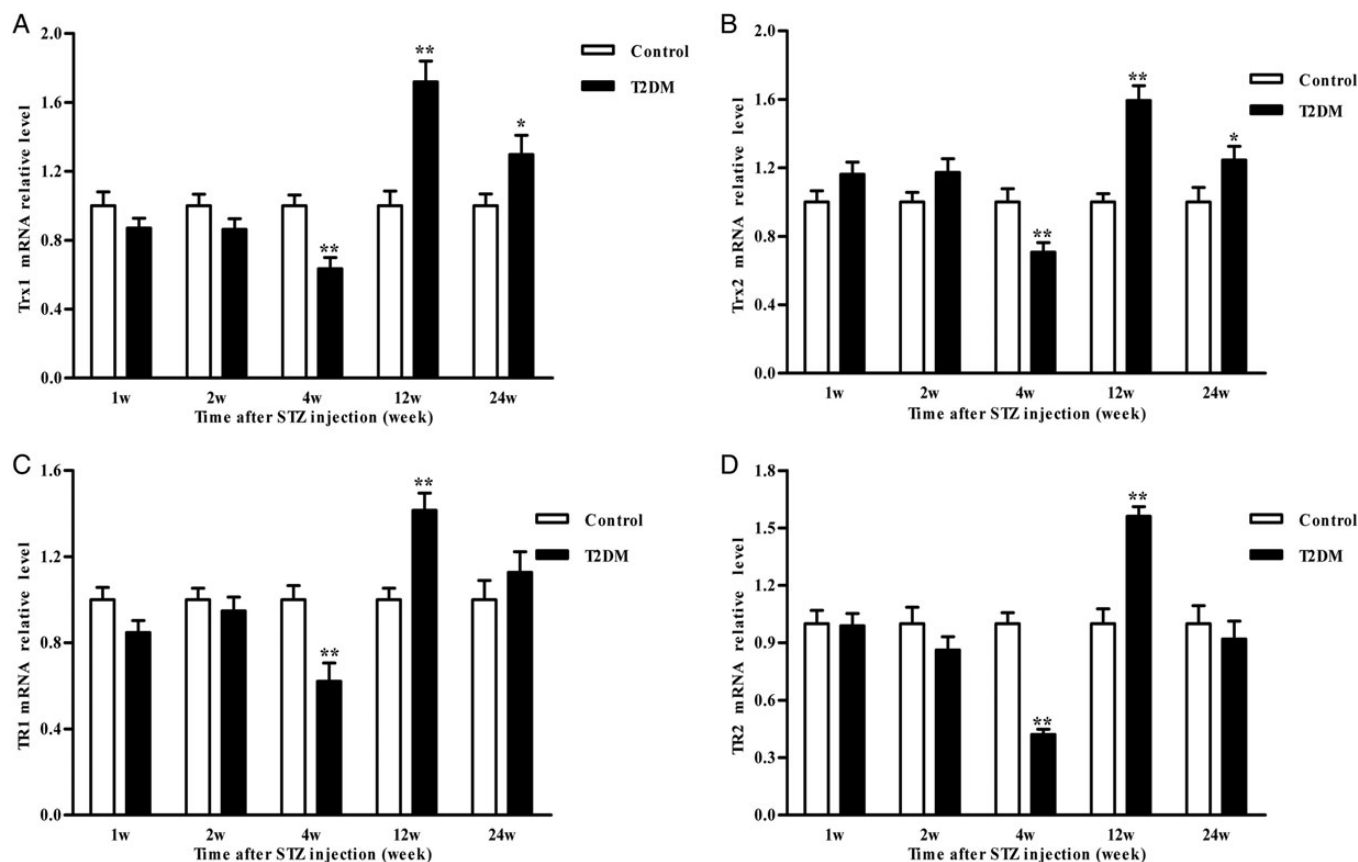


**Figure 3.** mRNA levels of *Trx* and *TR* in myocardial tissue detected by real-time PCR (A) *Trx1*; (B) *Trx2*; (C) *TR1*; (D) *TR2*. Trx, thioredoxin; TR, Trx reductase. All values are expressed as the mean  $\pm$  SD. In the T2DM group at week 24,  $n = 6$ ; and in the other groups,  $n = 10$ . \* $P < 0.05$ , \*\* $P < 0.01$  vs. control group.

### Trx nitration was increased, while Trx/ASK1 interaction was inhibited, and p38 activity was increased in the T2DM heart

Our recent study has demonstrated that Trx is susceptible to nitrative modification by peroxynitrite, and its activity is irreversibly inhibited by this novel post-translational modification [12]. To determine whether reduced Trx activity observed in the T2DM heart is caused by the increased Trx nitration, Trx nitration in normal and T2DM hearts was detected by immunoprecipitation (anti-Trx) followed by immunoblotting (anti-nitrotyrosine). As shown in **Fig. 5**, Trx nitration was not detected in cardiac tissues from control animals. In contrast, obvious Trx nitration was detected in cardiac tissues from the T2DM heart at the 12th week.

Recent *in vitro* studies have demonstrated that binding/inhibition of Trx with ASK1 is the primary mechanism by which Trx exerts its anti-apoptotic effect [24]. Moreover, the ratio of ASK1/Trx-ASK1 has been shown to be significantly increased in aged mouse livers, and this is correlated with the increased basal activity of the p38 MAPK pathway [25]. While determining whether Trx nitration may alter the Trx/ASK1 interaction, thereby activating the downstream pro-apoptotic kinases, two additional observations were made. As shown in **Fig. 6**, Trx is physically associated with ASK1

(anti-Trx-1 immunoprecipitation and anti-ASK1 immunoblotting) in cardiac tissues isolated from control animals, and this protein/protein interaction was significantly decreased in the T2DM animals at the 12th week (**Fig. 5B**). Consequently, the activity of p38, a pro-apoptotic downstream molecule for ASK1, was significantly enhanced in the T2DM heart compared with the control heart at the 12th week (**Fig. 7**).

### The change of mRNA and protein expression levels of TXNIP in the T2DM heart

TXNIP is the only currently known endogenous Trx inhibitory protein. TXNIP may bind with Trx and then the bound Trx loses the function of inhibiting cell apoptosis. As shown in **Fig. 8A**, compared with those of the control group, the mRNA expression of *TXNIP* in the T2DM group was significantly increased at the 4th, 12th, and 24th week. Moreover, the protein expression of TXNIP in the T2DM group was significantly increased at the 12th week (**Fig. 8B**).

## Discussion

T2DM is a complex, heterogeneous, and polygenic disease. Various types of animal models of T2DM either derived spontaneously or were induced by treating with chemicals,

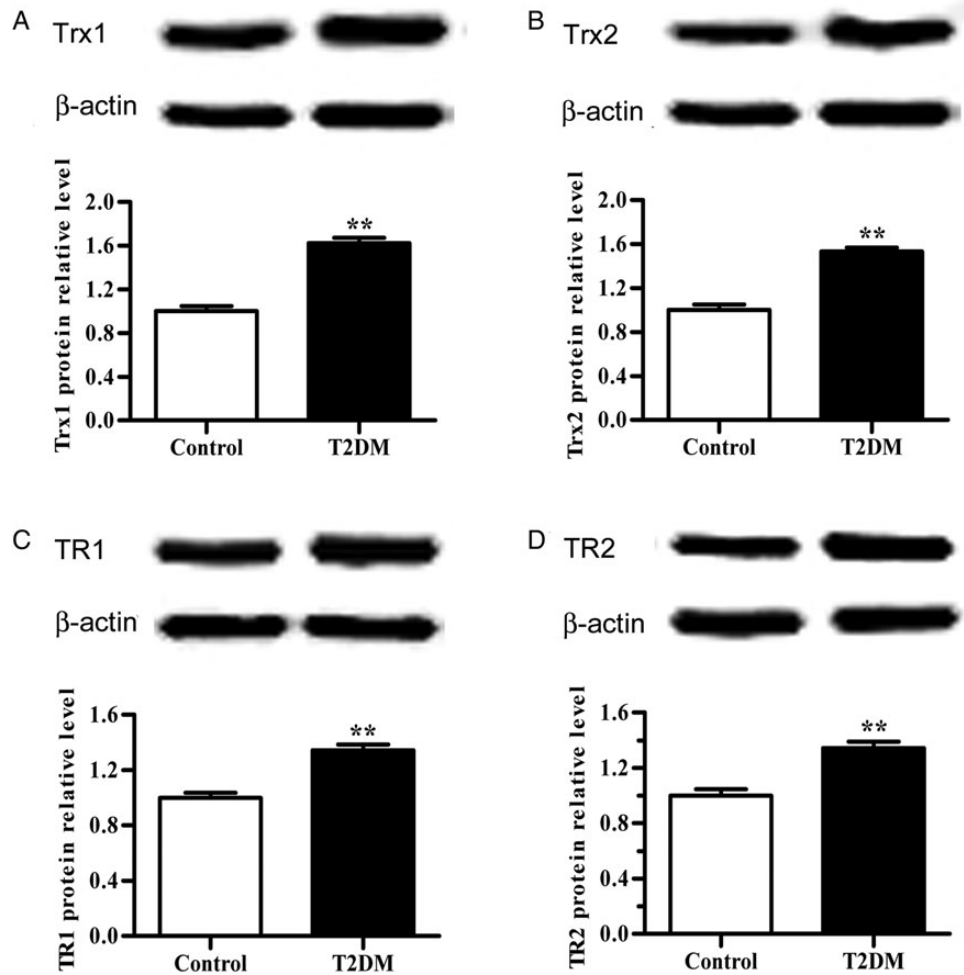


**Figure 4.** Levels of Trx and TR protein expression in myocardial tissue at week 12 after STZ injection (A) Trx1; (B) Trx2; (C) TR1; (D) TR2. Trx, thioredoxin; TR, Trx reductase. All values are expressed as the mean  $\pm$  SD,  $n = 6$ . \*\* $P < 0.01$  vs. control group.

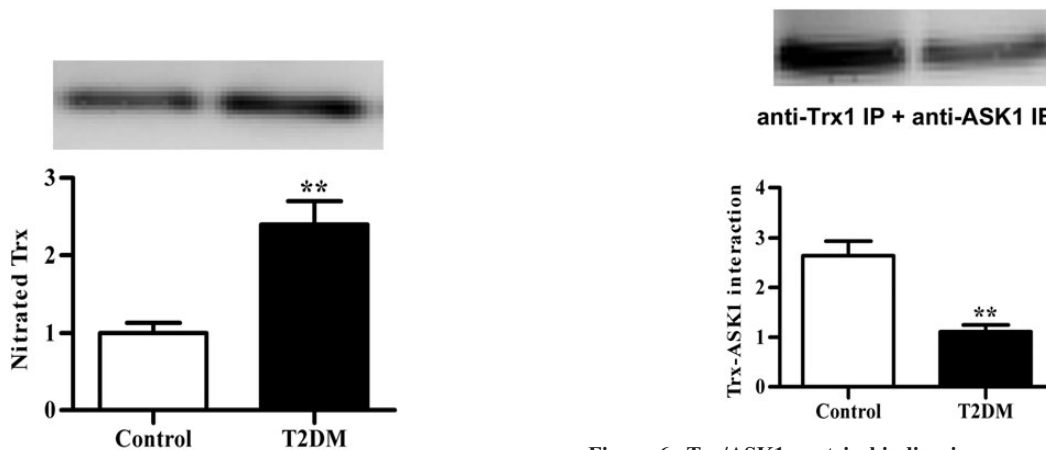


**Figure 5.** Trx nitration in myocardial tissue at week 12 after STZ injection. Trx nitration was detected by immunoprecipitation method. IP: anti-Trx monoclonal antibody, IB: anti-nitrotyrosine monoclonal antibody. All values are expressed as the mean  $\pm$  SD,  $n = 6$ . \*\* $P < 0.01$  vs. control group.

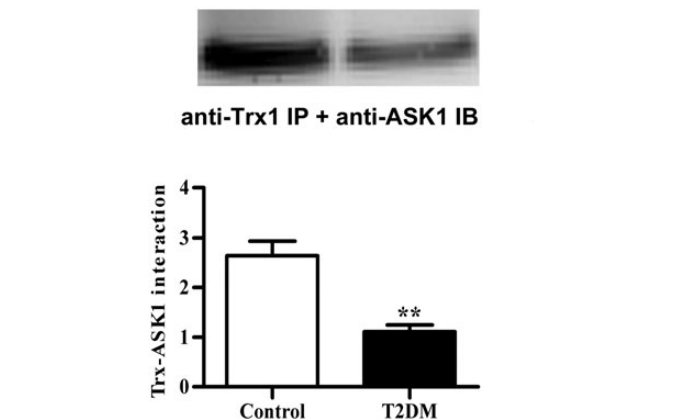


**Figure 6.** Trx/ASK1 protein binding in myocardial tissue at week 12 after STZ injection. Trx/ASK1 protein binding was detected by immunoprecipitation method. IP: anti-Trx monoclonal antibody, IB: anti-ASK1 polyclonal antibody. Trx, thioredoxin; ASK1, apoptosis signal regulating kinase 1. All values are expressed as the mean  $\pm$  SD,  $n = 6$ . \*\* $P < 0.01$  vs. control group.



or dietary or surgical manipulations. Furthermore, new animal models developed in the recent years by transgenic and knock-out mice are very expensive in diabetes research. Currently, many studies have reported that high-sugar and high-fat diet feeding animals develop insulin resistance [26–28]. At the same time, low-dose STZ has been known to induce a mild impairment of insulin secretion that is similar to the feature of the later stage of T2DM [29,30]; however, the injection dose of STZ (25, 30, 35, 40, and 45 mg/kg, i.p., respectively) and its methodologies were not consistent in those studies. In the present study, we chose a combination of high-fat diet with 40 mg/kg STZ injection to mimic the natural process and metabolic characteristics of T2DM in humans. After high-sugar and high-fat diet and STZ injection for 1 week, the level of blood glucose in rats of the T2DM group became significantly higher than that of the control group; meanwhile, the serum insulin level of the

T2DM group was not significantly changed or even higher than that of the control group. This suggested that the non-insulin-dependent T2DM rat model was successfully established [31].

Cardiac complications are the leading cause of death in diabetic patients. In this study, by measuring the cardiac function *in vivo*, we found that the levels of LVSP,  $+dP/dt_{max}$ , and  $-dP/dt_{max}$  in diabetic rats were significantly decreased from the 12th week, and the results indicated that the pump function of the heart was injured. Plasma biochemical indicators of myocardial injury such as CK-MB and cTnI levels were even elevated from the fourth week, which suggested that myocardial injury may occur in the early stage of diabetes. These parameters were aggravated with the disease progression, and would eventually lead to heart pump dysfunction and heart failure. The mechanism by which diabetes induces myocardial injury is still unclear. Considering that chronic and weak stimulations tend to induce apoptosis, our study mainly focused on cardiomyocyte apoptosis. A clinical research performed by Frustaci *et al.* [7] with ventricular myocardial biopsies obtained from diabetic patients proved that cardiomyocytes apoptosis were 85 folds higher than necrosis. In the present study, our results showed that caspase-3 activity was significantly increased from the 4th week in diabetic rats, and a significantly high number of TUNEL-positive cells were observed in the myocardial tissues from the 12th week in diabetic rats, indicating that diabetes can elicit myocardial apoptosis. Myocardial cells are terminally differentiated cells and cannot regenerate, so the continuous apoptosis induced by diabetes will inevitably reduce cardiomyocyte number and impair cardiac function.

Many pathways can induce apoptosis, among them the most important ones are the caspase-8 and the caspase-9-

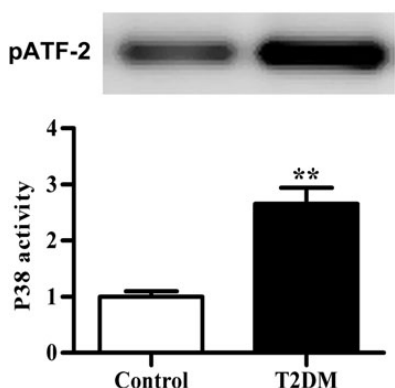


**Figure 7. p38 MAPK activity in myocardial tissue at week 12 after STZ injection** pATF2, phosphorylated activating transcription factor 2. All values are expressed as the mean ± SD,  $n = 6$ . \*\* $P < 0.01$  vs. control group.

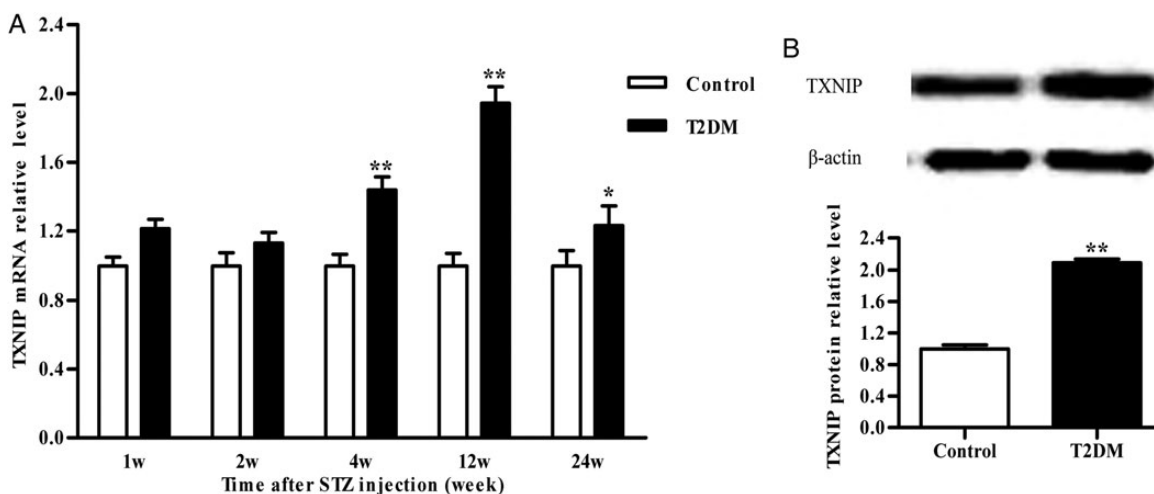


**Figure 8. Levels of TXNIP mRNA and protein expression in myocardial tissue** (A) Quantitative analysis for TXNIP mRNA level by real-time PCR. In the T2DM group at week 24,  $n = 6$ ; and in the rest groups,  $n = 10$ . (B) Densitometry analysis for TXNIP protein by western blot analysis at week 12 after STZ injection. TXNIP, Trx interacting protein. All values are expressed as the mean ± SD,  $n = 6$ . \* $P < 0.05$ , \*\* $P < 0.01$  vs. control group.

dependent apoptotic pathways. The caspase-8-dependent pathway which is mainly mediated by inflammatory mediators such as tumor necrosis factor- $\alpha$  (TNF- $\alpha$ ), starts apoptosis by activating caspase-8 through the interaction with its receptor, and is common in a variety of diseases including tumors, inflammation, and trauma [32]. However, the caspase-9-dependent pathway is usually involved in disease processes having lots of free radicals production such as reperfusion injury. As for diabetes, its marked hyperglycemia and hyperlipidemia induced by absolute or relative insulin deficiency evokes a lot of free radical generation and then induces cell apoptosis through caspase-9-dependent pathway [33]. Meanwhile, diabetes is regarded as an inflammatory process with the production of inflammatory mediators such as TNF- $\alpha$  and interleukin-6 [34], therefore, it would also initiate a caspase-8-dependent apoptotic pathway. Our results showed that the activity of caspase-8 was significantly increased from the 4th week in diabetic rats, while the activity of caspase-9 was significantly increased from the 12th week. Since both caspase-8 and caspase-9 locate in the upstream of caspase-3, we speculated that cardiomyocyte apoptosis is mainly induced through caspase-8- and caspase-9-dependent apoptotic pathways in diabetes, and caspase-8-dependent pathway precedes caspase-9-dependent pathway.

Trx system is a highly conserved protein system which widely exists in all life forms from lower bacteria to higher mammals, including humans [35,36]. Its family consisted of Trx, TR, and Trx peroxidase. Trx has two configurations: oxidized Trx (Trx-S<sub>2</sub>) and reduced Trx [Trx-(SH)<sub>2</sub>]. The reduced Trx may be transformed into oxidized Trx in the progress of scavenging free radicals. Under the action of the TR, the oxidized Trx may get electrons from NADPH and return to reduced Trx. Both Trx and TR have two subtypes. Trx1 and TR1 mainly exist in the cytoplasm, while Trx2 and TR2 mainly exist in the mitochondria. TR and Trx form an effective free radical scavenging system. Besides its antioxidant role, Trx was also reported to have important anti-apoptotic effects. Trx can bind to an important intracellular pro-apoptotic protein, ASK1, thus inhibiting ASK1 activity and the subsequent ASK1-dependent apoptotic pathway. In view of the important role of Trx in antioxidants and anti-apoptosis, we speculated that Trx might be involved in the occurrence of cardiomyocytes apoptosis caused by T2DM. In this study, myocardial Trx activity was significantly decreased in diabetic rats and this phenomenon aggravated gradually with the progression of disease. When Trx is inhibited, it will lose its ability to bind with ASK1, and then the freed ASK1 will activate its downstream protein target, JNK and p38 kinase, the two important pro-apoptotic proteins. In the present study, we also detected Trx-ASK1 interaction by immunoprecipitation method. The interaction of Trx and ASK1 was significantly decreased in the diabetic group, while p38 kinase activity was increased. The

interactions among Trx, ASK1, p38 kinase, and apoptosis have been shown in many studies of ischemia/reperfusion injury [37,38]. Besides, Trx inhibition may also elicit aggravated free radical damage which could be another reason for cardiomyocyte apoptosis found in diabetes, reperfusion injury, and other diseases.

According to our knowledge about Trx, the reasons for the decreased Trx activity in diabetes would be: (i) the expression level of Trx is reduced. In the present study, we found that the expression of myocardial Trx1 and Trx2 are decreased at the early stage of diabetes, partly accounting for the decline of its functions. However, at the later stage (after the 12th week), their expression was increased, which may be a compensatory response to decreased function of Trx system and increased free radical production. So, there must be other factors at this stage responsible for the declined Trx function; (ii) decreased activity of TR impedes the process or cycle of oxidized Trx back to reduced form. In this study, we determined the activity and expression of TR. Our results showed that myocardial TR activity was significantly decreased. This will break the Trx regenerative cycle and reduce the ratio of reduced Trx, and thus inhibit Trx activity or its function. TR expression was also decreased at the early stage of diabetes and increased again at later stage, just like the change of Trx. (iii) Nitration modification of Trx. It has been reported that ONOO<sup>-</sup> produced in reperfusion injury can induce Trx nitration at tyrosine<sup>49</sup>. The nitrated Trx will lose its ability to bind with ASK1 and then apoptosis was increased [11]. Our previous studies showed that there were large amount of nitric oxide and superoxide anion generated simultaneously in diabetic heart and they could rapidly react with each other to produce ONOO<sup>-</sup> and subsequently result in protein nitration. In this study, we detected Trx nitration directly by immunoprecipitation method. Our studies showed that Trx nitration was significantly increased in the diabetic group compared with control animals. (iv) Trx was inhibited by other endogenous proteins, such as TXNIP (Fig. 9).

TXNIP, also called (Trx binding protein 2) is the only known endogenous Trx regulatory protein. When bound with TXNIP, Trx will lose its ability to inhibit cell apoptosis. In this study, our results showed that TXNIP expression was significantly increased in the diabetic rat hearts, at both mRNA level and protein level. This is consistent with other reports in many types of cells including cardiomyocytes [39], and even in human diabetes [40]. High glucose has been identified as an important trigger of TXNIP up-regulation. Some researchers suggested that glucose can augment TXNIP transcription through a unique carbohydrate response element (ChoRE) in TXNIP promoter area [41]. Another candidate is p38 kinase. Recently, Su *et al.* [42] have proved that hyperglycemia enhances myocardial TXNIP expression, possibly through reciprocally modulating p38

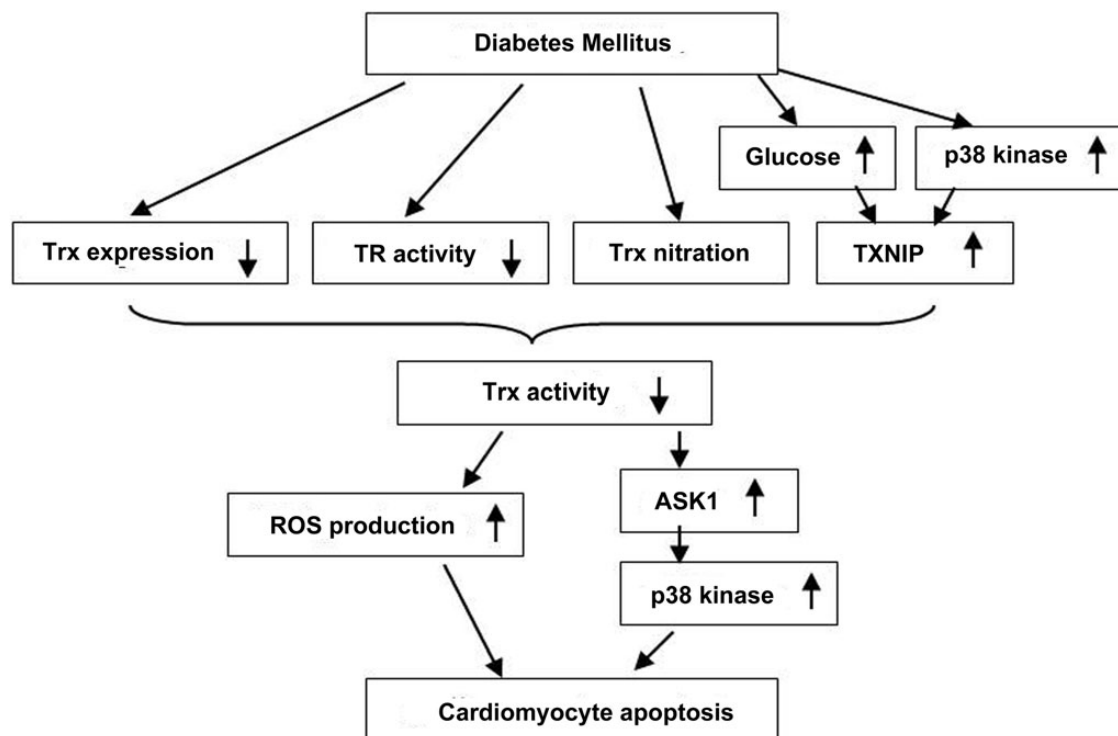


**Figure 9.** Trx system and diabetes-induced cardiomyocytes apoptosis

Trx, thioredoxin; TR, Trx reductase; TXNIP, Trx interacting protein; ASK1, apoptosis signal regulating kinase 1; ROS, reactive oxygen species.

MAPK and Akt activation. According to their report, p38 kinase is located at the upstream of TXNIP, which is proposed by other groups [12]. However, it has also been proved that TXNIP binds to and inhibits Trx, Trx binds to and inhibits ASK1 activation, and ASK1 is an upstream kinase of p38 kinase. The best explanation will be that p38 kinase may play roles both in TXNIP upstream and Trx downstream.

In the present study, we detected the expressions of Trx1 and TR1 in the cytoplasm, the expressions of Trx2 and TR2 in the mitochondria, respectively. The results showed that there was no obvious difference of Trx and TR expression between the cytoplasm and the mitochondria. Further studies are needed to ascertain whether there are still some differences of the Trx system between the cytoplasm and the mitochondria.

In conclusion, our findings showed that diabetes may attenuate the anti-apoptotic function of Trx by decreasing TR activity, inducing Trx nitration, up-regulating TXNIP expression, and down-regulating Trx expression in the early stage, and then induce cardiomyocytes apoptosis and heart injury.

## Funding

This work was supported by the grants from the National Natural Science Foundation of China (30800399), Scientific and Technological Foundation for Distinguished Returned

Overseas Chinese Scholars, Shanxi Province, China [2010(97)], and Innovation Talents Support Program of Universities, Shanxi Province, China.

## References

- Song SH. Emerging type 2 diabetes in young adults. *Adv Exp Med Biol* 2012, 771: 51–61.
- Chen AH and Tseng CH. The role of triglyceride in cardiovascular disease in Asian patients with type 2 diabetes, a systematic review. *Rev Diabetes Stud* 2013, 10: 101–109.
- Greer JJ, Ware DP and Lefer DJ. Myocardial infarction and heart failure in the db/db diabetic mouse. *Am J Physiol Heart Circ Physiol* 2006, 290: H146–H153.
- Chowdhry MF, Vohra HA and Galiñanes M. Diabetes increases apoptosis and necrosis in both ischemic and nonischemic human myocardium: role of caspases and poly-adenosine diphosphate-ribose polymerase. *J Thorac Cardiovasc Surg* 2007, 134: 124–131.
- Pennington JD, Jacobs KM, Sun L, Bar-Sela G, Mishra M and Gius D. Thioredoxin and thioredoxin reductase as redox-sensitive molecular targets for cancer therapy. *Curr Pharm Des* 2007, 13: 3368–3377.
- Li H, Wan A, Xu G and Ye D. Small changes huge impact: the role of thioredoxin 1 in the regulation of apoptosis by S-nitrosylation. *Acta Biochim Biophys Sin* 2013, 45: 153–161.
- Frustaci A, Kajstura J, Chimenti C, Jakoniuk I, Leri A, Maseri A and Nadal-Ginard B, *et al.* Myocardial cell death in human diabetes. *Circ Res* 2000, 87: 1123–1132.
- Tao L, Gao E, Hu A, Coletti C, Wang Y, Christopher TA and Lopez BL, *et al.* Thioredoxin reduces post-ischemic myocardial apoptosis by reducing oxidative/nitrative stress. *Br J Pharmacol* 2006, 149: 311–318.

9. Liu Y and Min W. Thioredoxin promotes ASK1 ubiquitination and degradation to inhibit ASK1-mediated apoptosis in a redox activity-independent manner. *Circ Res* 2002, 90: 1259–1266.
10. Nishida K and Otsu K. The role of apoptosis signal-regulating kinase 1 in cardiomyocyte apoptosis. *Antioxid Redox Signal* 2006, 8: 1729–1736.
11. Zhang H, Tao L, Jiao X, Gao E, Lopez BL, Christopher TA and Koch W, *et al.* Nitrate thioredoxin inactivation as a cause of enhanced myocardial ischemia/reperfusion injury in the aging heart. *Free Radic Biol Med* 2007, 43: 39–47.
12. Tao L, Jiao X, Gao E, Lau WB, Yuan Y, Lopez B and Christopher T, *et al.* Nitrate inactivation of thioredoxin-1 and its role in postischemic myocardial apoptosis. *Circulation* 2006, 114: 1395–1402.
13. Arambašić J, Mihailović M, Uskoković A, Dinić S, Grdović N, Marković J and Poznanović G, *et al.* Alpha-lipoic acid upregulates antioxidant enzyme gene expression and enzymatic activity in diabetic rat kidneys through an O-GlcNAc-dependent mechanism. *Eur J Nutr* 2012, 51: 975–986.
14. Fang KY, Shi MJ, Xiao Y, Gui HZ, Guo B and Zhang GZ. p38 MAPK mediates high glucose-induced renal tubular epithelial-mesenchymal transition. *Acta Physiol Sin* 2008, 60: 759–766.
15. Wang K, Zhang J, Liu J, Tian J, Wu Y, Wang X and Quan L, *et al.* Variations in the protein level of Omi/HtrA2 in the heart of aged rats may contribute to the increased susceptibility of cardiomyocytes to ischemia/reperfusion injury and cell death: Omi/HtrA2 and aged heart injury. *Age* 2013, 35: 733–746.
16. Wang XL, Liu HR, Tao L, Liang F, Yan L, Zhao RR and Lopez BL, *et al.* Role of iNOS-derived reactive nitrogen species and resultant nitrate stress in leukocytes-induced cardiomyocyte apoptosis after myocardial ischemia/reperfusion. *Apoptosis* 2007, 12: 1209–1217.
17. Zhao HX, Wang XL, Wang YH, Wu Y, Li XY, Lv XP and Zhao ZQ, *et al.* Attenuation of myocardial injury by postconditioning: role of hypoxia inducible factor-1 $\alpha$ . *Basic Res Cardiol* 2010, 105: 109–118.
18. Yamamoto M, Yang G, Hong C, Liu J, Holle E, Yu X and Wagner T, *et al.* Inhibition of endogenous thioredoxin in the heart increases oxidative stress and cardiac hypertrophy. *J Clin Invest* 2003, 112: 1395–1406.
19. Das KC, Guo XL and White CW. Induction of thioredoxin and thioredoxin reductase gene expression in lungs of newborn primates by oxygen. *Am J Physiol* 1999, 276: L530–L539.
20. Yoshida A, Suzuki N, Nakano Y, Oho T, Kawada M and Koga T. Development of a 5' fluorogenic nuclease-based real-time PCR assay for quantitative detection of *Actinobacillus actinomycetemcomitans* and *Porphyromonas gingivalis*. *J Clin Microbiol* 2003, 41: 863–866.
21. Tao L, Gao E, Bryan NS, Qu Y, Liu HR, Hu A and Christopher TA, *et al.* Cardioprotective effects of thioredoxin in myocardial ischemia and reperfusion: role of S-nitrosation. *Proc Natl Acad Sci USA* 2004, 101: 11471–11476.
22. Vadseth C, Souza JM, Thomson L, Seagraves A, Nagaswami C, Scheiner T and Torbet J, *et al.* Prothrombotic state induced by post-translational modification of fibrinogen by reactive nitrogen species. *J Biol Chem* 2004, 279: 8820–8826.
23. Gao F, Yue TL, Shi DW, Christopher TA, Lopez BL, Ohlstein EH and Barone FC, *et al.* p38 MAPK inhibition reduces myocardial reperfusion injury via inhibition of endothelial adhesion molecule expression and blockade of PMN accumulation. *Cardiovasc Res* 2002, 53: 414–422.
24. Saitoh M, Nishitoh H, Fujii M, Takeda K, Tobiume K, Sawada Y and Kawabata M, *et al.* Mammalian thioredoxin is a direct inhibitor of apoptosis signal-regulating kinase (ASK) 1. *EMBO J* 1998, 17: 2596–2606.
25. Hsieh CC and Papaconstantinou J. Thioredoxin-ASK1 complex levels regulate ROS-mediated p38 MAPK pathway activity in livers of aged and long-lived Snell dwarf mice. *FASEB J* 2006, 20: 259–268.
26. Zhao S, Chu Y, Zhang C, Lin Y, Xu K, Yang P and Fan J, *et al.* Diet-induced central obesity and insulin resistance in rabbits. *J Anim Physiol Anim Nutr* 2008, 92: 105–111.
27. Tanaka S, Hayashi T, Toyoda T, Hamada T, Shimizu Y, Hirata M and Ebihara K, *et al.* High-fat diet impairs the effects of a single bout of endurance exercise on glucose transport and insulin sensitivity in rat skeletal muscle. *Metabolism* 2007, 56: 1719–1728.
28. Flanagan AM, Brown JL, Santiago CA, Aad PY, Spicer LJ and Spicer MT. High-fat diets promote insulin resistance through cytokine gene expression in growing female rats. *J Nutr Biochem* 2008, 19: 505–513.
29. Reed MJ, Meszaros K, Entes LJ, Claypool MD, Pinkett JG, Gadbois TM and Reaven GM. A new rat model of type 2 diabetes: the fat-fed, streptozotocin-treated rat. *Metabolism* 2000, 49: 1390–1394.
30. Srinivasan K, Viswanad B, Asrat L, Kaul CL and Ramarao P. Combination of high-fat diet-fed and low-dose streptozotocin-treated rat: a model for type 2 diabetes and pharmacological screening. *Pharmacol Res* 2005, 52: 313–320.
31. Chatzigeorgiou A, Halapas A, Kalafatakis K and Kamper E. The use of animal models in the study of diabetes mellitus. *In Vivo* 2009, 23: 245–258.
32. Liedtke C and Trautwein C. The role of TNF and Fas dependent signaling in animal models of inflammatory liver injury and liver cancer. *Eur J Cell Biol* 2012, 91: 582–589.
33. Cheng B, Pan S, Liu X, Zhang S and Sun X. Cell apoptosis of taste buds in circumvallate papillae in diabetic rats. *Exp Clin Endocrinol Diabetes* 2011, 119: 480–483.
34. Das J and Sil PC. Taurine ameliorates alloxan-induced diabetic renal injury, oxidative stress-related signaling pathways and apoptosis in rats. *Amino Acids* 2012, 43: 1509–1523.
35. Yamawaki H, Haendeler J and Berk BC. Thioredoxin: a key regulator of cardiovascular homeostasis. *Circ Res* 2003, 93: 1029–1033.
36. Hirota K, Nakamura H, Masutani H and Yodoi J. Thioredoxin superfamily and thioredoxin-inducing agents. *Ann NY Acad Sci* 2002, 957: 189–199.
37. Yin T, Hou R, Liu S, Lau WB, Wang H and Tao L. Nitrate inactivation of thioredoxin-1 increases vulnerability of diabetic hearts to ischemia/reperfusion injury. *J Mol Cell Cardiol* 2010, 49: 354–361.
38. Luan R, Liu S, Yin T, Lau WB, Wang Q, Guo W and Wang H, *et al.* High glucose sensitizes adult cardiomyocytes to ischemia/reperfusion injury through nitrate thioredoxin inactivation. *Cardiovasc Res* 2009, 83: 294–302.
39. Chen J, Cha-Molstad H, Szabo A and Shalev A. Diabetes induces and calcium channel blockers prevent cardiac expression of proapoptotic thioredoxin-interacting protein. *Am J Physiol Endocrinol Metab* 2009, 296: E1133–E1139.
40. Parikh H, Carlsson E, Chutkow WA, Johansson LE, Storgaard H, Poulsen P and Saxena R, *et al.* TXNIP regulates peripheral glucose metabolism in humans. *PLoS Med* 2007, 4: e158.
41. Minn AH, Hafele C and Shalev A. Thioredoxin-interacting protein is stimulated by glucose through a carbohydrate response element and induces beta-cell apoptosis. *Endocrinology* 2005, 146: 2397–2405.
42. Su H, Ji L, Xing W, Zhang W, Zhou H, Qian X and Wang X, *et al.* Acute hyperglycaemia enhances oxidative stress and aggravates myocardial ischemia/reperfusion injury: role of thioredoxin-interacting protein. *J Cell Mol Med* 2013, 17: 181–191.